Environmental Science
Water Research & Technology

PAPER

View Article Online
View Journal | View Issue

Cite this: *Environ. Sci.: Water Res. Technol.*, 2025, **11**, 1339

Novel fluidized-bed bioreactors with density-graded carriers for the bioremediation of nitrate in uranium industry effluents

Mariano Venturini,[a] Paula Bucci *[b] and Raúl Muñoz[b]

Received 23rd January 2025,
Accepted 31st March 2025

DOI: 10.1039/d5ew00077g

rsc.li/es-water

This study presents an innovative bioreactor system that employs density-graded floating carriers to effectively remediate complex uranium-contaminated effluents generated by the nuclear industry. By combining the advantages of fixed-bed and fluidized-bed reactors, our system utilizes floating carriers to create a stratified biofilm environment, optimizing biomass retention and mass transfer. Controlled redox potential (ORP) enhances the removal of uranium and associated contaminants, especially in effluents with high-nitrate concentrations. The fluidized-bed configuration, with a high carrier load, minimizes biofilm-induced clogging, ensuring sustained performance. Carriers were synthesized with acrylate polymers in different compositions: HEMA 50%/0 AA, HEMA 50%/25% AA and HEMA 50%/50% AA w/w to obtain different hydrodynamic properties. The particle terminal velocities and drag coefficients of carriers were 3.14×10^{-6} m s^{-1}, 5×10^{-5} m s^{-1}, and 2×10^{-4} m s^{-1} and 661 976, 20 734, and 26 221, respectively. The system achieved nitrate and COD removal efficiencies of up to 90% and 84%, respectively, at a hydraulic retention time of 23.9 h and with low energy consumption. The system behaved like a fluidized bed with a high carrier load similar to the PBBR, showing piston flux and variable column fluidization based on carrier densities. Frictions and collisions prevented clogging due to biofilm formation, ensuring sustained performance.

Water impact

Water is an essential resource, and its quality is directly linked to the health of ecosystems and human communities. Our manuscript, "*Novel Fluidized-Bed Bioreactors with Density-Graded Carriers for the Bioremediation of Nitrate in Uranium Industry Effluents*", highlights the crucial role that advanced wastewater treatment technologies can play in addressing current water sustainability challenges, particularly in the nuclear industry. High-nitrate effluents from nuclear processes pose significant risks to both environmental and public health, contaminating water sources and disrupting ecosystems. Our research presents a novel approach to treating these complex wastewater streams by using density-graded floating carriers to optimize bioreactor performance. The impact of our research on water sustainability is multifaceted: 1. **Water quality improvement**: our bioreactor system offers a sustainable and efficient solution for reducing nitrate levels in high-nitrate wastewater, ensuring cleaner and safer water for both environmental and human use. 2. **Ecosystem protection**: by efficiently removing harmful contaminants such as nitrates, our system helps preserve the integrity of aquatic ecosystems, preventing eutrophication and supporting biodiversity in water bodies. 3. **Environmental sustainability**: the use of floating carriers in a fluidized bed bioreactor minimizes energy consumption and chemical additives, contributing to the development of low-impact, resource-efficient wastewater treatment technologies. 4. **Innovation in water treatment**: our research demonstrates the innovative potential of density-graded floating carriers in wastewater treatment, setting a new precedent for the design of high-performance, sustainable bioreactor systems capable of handling complex industrial effluents. In conclusion, our manuscript underscores the importance of innovative and sustainable solutions for treating high-nitrate wastewater, offering a path forward for improving water quality, protecting ecosystems, and advancing the goal of water sustainability. We believe that sharing our findings in *Environmental Science: Water Research & Technology* will catalyze further research and inspire the development of advanced, eco-friendly water treatment technologies for industrial applications.

1 Introduction

To produce nuclear fuels, uranium ore must be converted into ceramic-grade UO_2, and the process involves the use of various substances such as kerosene, methanol, nitric acid, ammonia, and to a lesser extent, tributyl phosphate (TBP). The characterization of the effluents generated reveals the presence of uranium typically ranging from 300–600 mg L^{-1} as U–U_3O_8, kerosene and methanol at levels of 900–1600 mg L^{-1} as COD, and nitrogen compounds up to 1500 mg L^{-1} as N–NO_3^-. High-

[a] *Biomining and Environmental Biotechnology Laboratory – National Commission of Atomic Energy, Av. Ptero González y Aragón No. 15, B1802AYA, Buenos Aires, Argentina*
[b] *Institute of Sustainable Processes, University of Valladolid, Doctor Mergelina s/n, 47011, Valladolid, Spain. E-mail: paulalorena.bucci@uva.es*

nitrate concentrations contribute to eutrophication, while uranium poses risks of radioactive contamination. Strict environmental regulations mandate effective treatment to minimize emissions and ensure compliance.

Conventional treatment methods, such as reverse osmosis, evaporation, and electrodialysis, can achieve high-nitrate removal efficiencies above 82% at 1000 mg L^{-1} $N\text{–}NO_3^-$. Uranium-contaminated effluents pose a significant challenge in the nuclear industry. Treatment methods such as zero liquid discharge (ZLD) processes rely on energy-intensive thermal operations such as evaporation and crystallization, resulting in high operational costs. In contrast, the system proposed in this study employs a biological approach that avoids thermal operations, suggesting a potential advantage in terms of energy efficiency and operational costs. In addition, ZLD requires the use of corrosion-resistant materials, such as high-grade stainless steels, due to the highly corrosive nature of the effluents. This work focuses on the kinetics of nitrate removal from nuclear effluents, providing a sustainable alternative to conventional methods.[1–4]

Other methods often require extensive pretreatment stages (ultrafiltration, microfiltration, and sand filtration) and incur high operating costs, limiting their sustainability for *e.g.* the use of IONAC SR-7 coupled with reverse osmosis.[5,6] Additional approaches such as supercritical water treatment at 374 °C, electrochemical methods, and electrodialysis are effective yet associated with high energy demands and potential NOx emissions.[7,8]

Biological treatment methods provide promising and economically viable alternatives, particularly for high-nitrate and COD effluents in the uranium industry. Anaerobic biotechnologies excel at nitrate and COD removal under controlled conditions.[9,10] Biofilm-based reactors provide advantages such as robustness and tolerance to environmental variations. However, conventional biofilm reactors are susceptible to clogging, which limits mass transfer and hydrodynamic efficiency. To address these challenges, this study proposes a hybrid bioreactor system that combines the benefits of packed-bed and fluidized-bed reactors using density-graded hydrogel carriers.[11–13] These issues necessitate bioreactor designs that minimize clogging and maximize mass transfer, ensuring effective treatment of uranium-contaminated effluents with high nitrate and COD concentrations.

Two major types of anaerobic biofilm bioreactors are widely used for industrial wastewater treatment: packed-bed bioreactors (PBBRs) and fluidized-bed bioreactors (FBBRs). PBBRs immobilize cells within stationary packing materials such as plastic or ceramic rings, facilitating biofilm formation and enhancing mass transfer. PBBRs typically operate under laminar flow conditions, characterized by smooth, orderly fluid motion that maximizes contact between the fluid and the biofilm. However, laminar flow can also lead to clogging and dead zones, reducing treatment efficiency. In contrast, FBBRs suspend biofilm-attached carriers in a fluid, maintaining biofilm suspension through fluid velocity. Turbulence is quantified using the Reynolds number, which must exceed a minimum threshold to ensure fluidization of the carriers and the liquid phase.

This configuration enables uniform particle mixing and continuous operation, reducing clogging due to biofilm accumulation. FBBRs have been shown to offer higher resistance to system disturbances and greater resilience to load fluctuations, enhancing long-term hydrodynamic stability and biofilm growth even under varying influent conditions.[14–16] FBBRs generally require larger reactor volumes, higher pumping capacity, and greater energy inputs due to the fluidization requirements. Additionally, particle entrainment can affect their efficiency and scalability.

To overcome these limitations, FBBRs can be modified with specific biofilm carriers that optimize treatment efficiency while maintaining fluidization. Numerous commercially available carriers, including polyethylene, polypropylene, and biopolymer-based options, are designed with variations in density, shape, and buoyancy to suit specific applications. Methacrylate hydrogels are particularly promising carriers due to their ability to copolymerize with amides, creating carriers with variable densities and buoyancy characteristics.[17–20] This flexibility supports hybrid bioreactor configurations that combine the mass transfer benefits of FBBRs with the surface area advantages of PBBRs, addressing limitations related to clogging and hydrodynamics.

We hypothesize that by employing density-graded hydrogel carriers within a fluidized-bed reactor, we can create a stratified biofilm environment, aimed at the advantages of a packed bed while mitigating the risk of clogging. This hybrid approach achieves high biomass retention and efficient mass transfer, characteristic of PBBRs, while maintaining the fluidization benefits and minimizing energy consumption associated with FBBR.

This study introduces a novel approach to bioreactor design by utilizing density-graded hydrogel carriers within a fluidized-bed configuration. This approach differs from conventional FBBRs by creating a stratified biofilm environment, giving the advantages of packed-bed reactors while maintaining the benefits of fluidization. The high nitrate and COD concentrations, combined with the presence of potentially inhibitory compounds, present significant challenges for the effective treatment of uranium-contaminated effluents.

Packed-bed and fluidized-bed reactors are widely used in chemical and biotechnology industries due to their advantages over suspended cell systems, particularly in wastewater treatment, where they demonstrate high resistance to disturbances such as inhibitors, pH fluctuations, and biomass loss.[21] While PBBRs typically operate under laminar flow, FBBRs predominantly function under turbulent conditions. This study contributes fundamental insights into laminar-regime FBBR hydrodynamics for nuclear wastewater treatment, emphasizing shear forces' role in balancing biofilm growth and detachment to prevent clogging. Strategic carrier selection and placement further enhance the reactor's

performance by optimizing biofilm growth and fouling control.[22,23]

Successful development of this hybrid bioreactor system has the potential to significantly advance the field of wastewater treatment, providing a more sustainable and cost-effective solution for the remediation of uranium-contaminated effluents and other challenging industrial waste streams. The proposed biological system operates at ambient temperature and pressure, eliminating the need for energy-intensive thermal operations. Additionally, the system can be constructed using durable plastics, which are less expensive and more resistant to corrosion than stainless steels. This represents a potential advantage in terms of both energy efficiency and capital costs.

2 Materials and methods

2.1 Blended real nuclear wastewater (BRNW)

The production of ceramic-grade UO_2 fuel begins with yellow cake, which is dissolved in nitric acid, purified, and precipitated using methanol and kerosene at uranium concentrations of up to 200 g L^{-1}. The final effluent from this process, known as blended real nuclear wastewater (BRNW), contains residual uranium (300–600 mg L^{-1} as U–U_3O_8), methanol, kerosene, and high-nitrate concentrations (1000–1300 mg L^{-1} as N–NO_3^-). This effluent was used in our experiments without additional pretreatment, except for pH adjustment and equalization to stabilize COD levels.[24,25] Real nuclear wastewater samples used in this study were obtained from an Argentinian uranium conversion facility. This blended real nuclear wastewater (BRNW) was characterized by the composition shown in Table 1. Prior to use, the effluent underwent an equalization process to stabilize the pH and COD levels, after which the resulting precipitate was discarded. The BRNW also contains methanol and kerosene as major organic contaminants. This industrial effluent, which includes contributions from domestic wastewater, is further treated with surfactant compounds to adjust the pH to 8.

2.2 Synthesis of hydrogel carriers

A range of carrier materials including biodegradable polymers (BDP), high-density polyethylene (HDPE), polyvinyl alcohol (PVA), polyurethane sponge (PS), and granular activated carbon (GAC) are currently employed in various types of bioreactors, such as moving-bed biofilm reactors (MBBRs) and fluidized-bed biofilm reactors (FBBRs). Commercial polymeric carriers such as Kaldness 5 and Saddle-Chips SC exhibit properties including a density of 0.96 kg m^{-3}, a surface area ranging from 800 to 700 m^3 m^{-3}, and varying porosity levels (65–87%).[26]

In the present study, acrylic materials (HEMA and AA) were chosen according to the properties of swelling (hydrogel) induced by gamma-radiation synthesis. The concept behind synthesizing hydrogels *via* gamma polymerization is to achieve carrier polymerization and sterilization simultaneously in a single step, eliminating the need for elevated temperatures and crosslinking agents that may exert a toxic influence on microorganisms. Additionally, the gradual addition of acrylamide imparts primary amino groups to the polymer, enhancing its swelling properties and consequently reducing density through volume expansion. HEMA was polymerized by gamma radiation and copolymerized with AA, which were purchased from Sigma (Aldrich, WI, USA). Following polymerization, the sample was homogenized and air was removed by bubbling with nitrogen. The samples were irradiated at 25 kgy (5 kgy h^{-1}) by ^{60}Co gamma-irradiation source at PISI – Centro Atómico Ezeiza (Argentina). The concentrations of HEMA (50%) and AA (25% and 50%) were chosen to optimize hydrogel properties. A 50% HEMA concentration balances the mechanical strength and flexibility, while AA concentrations ensure optimal swelling without compromising structural integrity. These choices enable the hydrogels to support biofilm growth and withstand fluidized-bed reactor conditions.

The swelling dynamic and equilibrium were determined by the Cuggino methodology.[27] The swelling rate (qw) was determined gravimetrically at different times using eqn (1a) and during the equilibrium using eqn (1b):

$$qw = mh/ms(1) \quad (1a)$$

$$qw = me/ms \quad (1b)$$

where mh is the swelled hydrogel (HG) mass at each time, me is the HG mass during the equilibrium, and ms is the dry HG mass. The HG carriers were hydrated, previously dried at 35 °C, and then, they are weighed in determined periods of time. This test finished when the carrier weight was stable in time (water equilibrium). This essay allowed determining the maximum weight and volume increase. The carriers were constructed with a cylindrical shape with 15 mm external diameter and 5 mm internal diameter with 20 mm length. Different concentrations of HEMA were tested: 50.0% v/v in water and the addition of AA 0, 25 and 50.0% (% V/V HEMA). The densities were decreased according to AA incorporation.

Table 1 Chemical composition of wastewater discharged from nuclear manufacturing industries

Parameter	Unit	Concentration
Ammonium	mg L^{-1}	600–1400 ± 32
Nitrate	mg L^{-1}	1000–1300 ± 36
COD	mg L^{-1}	1500 ± 38
pH		7.0–7.8
Uranium	mg L^{-1}	300–600 ± 24

2.3 Bioreactor configuration and operational mode

This study utilized a comparative approach to evaluate the performance of two bioreactor configurations: a packed-bed bioreactor (PBBR) and a fluidized-bed bioreactor (FBBR),[28] with

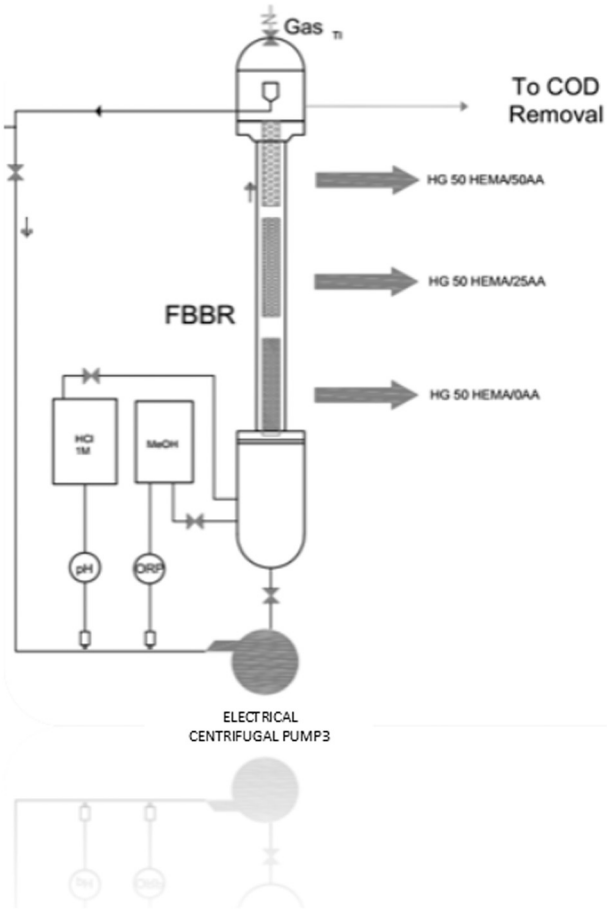

Fig. 1 Denitrification fluidized-bed bioreactor.

the aim of high biomass retention while minimizing energy consumption and hydrodynamic properties.

The PBBR was a single-unit, multi-layer fixed-bed reactor fabricated using polypropylene sheets. This configuration offers several advantages such as high volumetric organic removal rates and efficient liquid–solid separation. The FBBR was designed to optimize fluidization characteristics and minimize clogging.[15,16] This study comprehensively reviewed the fundamental aspects of FBBRs including their applications, configurations, and recent advancements in reactor performance.[29–31]

The FBBR was designed to optimize the fluidization characteristics and minimize clogging. To achieve this, the reactor was loaded with hydrogel carriers, exhibiting varying densities (50% p/p HEMA/AA, 25% p/p HEMA/AA, and HEMA only). This density gradient facilitated a stratified arrangement of carriers, promoting optimal biofilm growth while preventing clogging.

To facilitate comparison between systems of different scales, the hydraulic retention time (HRT) values were converted into dimensionless residence time units (RTUs) using the following equation, where the actual residence time (RT) was divided by the HRT. The reference time unit (t_0) can be chosen based on the characteristic time scale of the system, such as the average particle size or the reactor volume. The output values and the resulting plotted curves followed a logarithmic-type function of the form $Cs - \log Co \cdot e^{-a.tr}C$, where Cs is the output nitrate concentration, Co is the initial nitrate concentration, tr is the residence time, r is the radial position, and a is an experimental coefficient obtained using appropriate statistical methods.

The Peclet number (Pe) was calculated using the following standard equation for tubular systems:

$$Pe = (v \times L)/Dz$$

where v is the superficial velocity, L is the reactor length, and Dz is the axial dispersion coefficient. The dispersion coefficient was estimated from the response curve using the method of moments. The obtained Pe values indicated a predominant plug flow regime, with relatively low axial dispersion. This suggests that the reactor design promotes efficient conversion and minimal backmixing.

2.3.1 Fluidized-bed bioreactor (FBBR). To evaluate the impact of operating conditions on nitrate removal efficiency, experiments were conducted at different influent nitrate concentrations (1400, 2800, and 4200 mg L^{-1}) while maintaining a constant flow rate of 0.0029 L min^{-1}. This flow rate was selected to yield a Peclet number of 4, which has been previously determined to optimize the mass transfer within the reactor. To ensure effective denitrification under anaerobic conditions, methanol was added to the reactor through dosing based on a C/N ratio of 1.85 (Fig. 1 and Table 2). Continuous monitoring of nitrate and COD concentrations using ORP allowed for optimal denitrification

Table 2 Swelling of hydrogel and effects of AA into HEMA

Weight (g) (/% HEMA/% AA)										
H	50/0	SD ±	50/5	SD ±	50/10	SD ±	50/25	SD ±	50/50	SD ±
0.00	4.97	0.40	3.34	0.55	3.01	0.33	4.06	0.24	6.18	0.17
24.00	6.34	0.36	5.16	0.44	5.26	0.33	8.90	0.26	15.00	0.20
48.00	6.79	0.36	6.00	0.41	5.88	0.34	10.89	0.27	17.50	0.24
96.00	7.50	0.37	6.50	0.39	7.30	0.37	12.57	0.28	21.11	0.22
120.00	7.67	0.38	7.00	0.39	8.50	0.41	14.00	0.34	23.00	0.24
144.00	9.89	0.40	7.70	0.41	9.23	0.44	15.36	0.34	26.00	0.26
720.00	9.90	0.45	8.40	0.44	9.35	0.58	17.32	0.50	33.09	0.40
Qw	1.99		2.50		3.10		4.20		5.30	

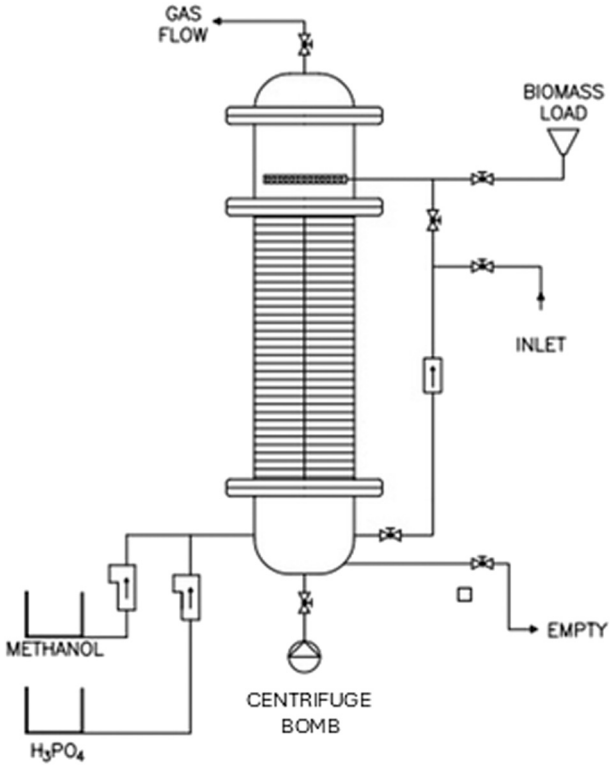

Fig. 2 Packed-bed bioreactor.

performance. The flow (Q) was 0.0029 l min^{-1}, Peclet number was $TRH^2/\sum T^{(1/2)}$, dispersion module = 1/Peclet number, and axial dispersion = flux × length/Peclet number. Nitrate was conducted to characterize the axial dispersion within the reactor. A step change in nitrate concentration was introduced, and the effluent was monitored over time. The time of peak concentration was used to determine the mean residence time, and the variance of the response curve was used to calculate the axial dispersion coefficient.

Three types of hydrogel carriers with varying densities (50% p/p HEMA/AA, 25% p/p HEMA/AA, and HEMA only) were used. The flow rate was carefully regulated using a valve to ensure optimal fluidization, preventing carrier escape from the top of the reactor while allowing for carrier mobilization. The distribution of carriers within the reactor was monitored over time. The average distribution and the minimum and maximum rise of each carrier type were determined.

2.3.2 Packed-bed bioreactors (PBBRs). The packed-bed bioreactor (Fig. 2) was constructed using a cylindrical acrylic column with a diameter of 20 cm and a height of 110 cm. Perforated polycarbonate plates were used to promote biofilm adhesion, with a diameter equivalent to that of the cylinder.

Polycarbonate (PC) was chosen as the packing material based on its rugged surface, which enhances biofilm adhesion and promotes stable microbial colonization, as supported by previous studies. While alternative materials were not tested in this study due to design constraints, the high denitrification efficiency achieved with PC confirms its suitability for PBBR applications.

Recirculation was achieved using a peristaltic pump operating at different speeds to produce downstream recirculation. A dosing pump was used to regulate the feed, while a hydraulic closure was employed to prevent oxygen entering the system from the outside.

In the analysis of the results, the values of HRT were converted to residence time unit (RTU), where de RT was divided by time. The output values and the resulting plotted curves followed a logarithmic-type function of the form log type $Cs - \log Co{\cdot}e^{-a.tr}$, where Cs is the nitrate concentration at the output, Co is the initial nitrate concentration, tr is the residence time, r is the radial position, and a is an experimental coefficient. The influence of nitrate concentration on the hydraulic retention time was evaluaded at levels of 125, 250, 500, 750, and 1000 mg l^{-1} $N\text{–}NO_3^-$ in PBBR.

2.3.3 Drag coefficient. The drag coefficient measures resistance to motion in a fluid, and interpretation depends on specific context. The equation is as follows:

$$C_D^* = \frac{432}{\varnothing_p}\left(1 + 0.047\varnothing_1^{\frac{2}{3}}\right) + \frac{0.517}{1 + 154\varnothing_1^{\frac{2}{3}}}$$

where

$$\varnothing_1^* = {d_p}^3 = \frac{4}{3}\frac{(\rho_s - \rho_l)\rho_1 g {d_p}^3}{{\mu_1}^2} \quad R^* = \left(\frac{\varnothing_1^*}{C_D^*}\right)^{1/2} \quad V_T = R^* \frac{\mu_1}{d_p \rho_l}$$

C_D^* = particle drag coefficient, d_p is the particle diameter (m), V_T is the terminal velocity (m s^{-1}), ρ_l is the fluid density (kg m^{-3}), ρ_p is the particle density (kg m^{-3}), R particle is the particle Reynolds number and μ_1 is the fluid viscosity.

2.4 Control of environmental conditions to monitor ORP

Nitrate concentrations were determined according to standardized methods (refer to the test analysis section for details).

The oxidation–reduction potential (ORP) in the system was modeled using the Nernst equation, as proposed by Chang and Venturini.[32,33] This model, based on the Nernst equation, describes the relationship between ORP and the concentrations of redox couples in the system, assuming a 1/1 stoichiometric ratio for each chemical reaction

$$NO_3^- + \frac{5}{6}CH_3OH \gg \frac{1}{2}N_2 + \frac{5}{6}CO_2 + \frac{7}{6}H_2O + OH^-$$

The standard potential ($E°$) used in this work was 154 mV for ammonium oxidation to nitrite (NO_2^-) and −340 mV for ammonium oxidation to nitrate E^0 (NO_3^-). The original equation was modified by replacing $\ln(1/[H^+])$ for 2.3026 × 4 pH according to the author:

$$E = E° + \frac{RT}{NF} \times \ln\left[\frac{(NH_4^+) \times (DO) \times (H_2O)}{(NO_x^-) \times (H)^{(8\text{ or }6)+}}\right] a_{ox}/a_{red}$$

where E is the potential activity of the reduced and oxidized

species, a_{Ox} and a_{Red}. E_0 is the standard potential: E_0 (NO_2^-) = 154 mV or E_0 (NO_3^-) = −340 mV. In applying the Nernst equation, it was assumed that the substrate concentration remained constant and in excess. Thus, the modified Nernst equation used in this work is expressed as follows:

$$E = -340\ \text{mV} + \left(\frac{0.059}{6} \times \log \text{DO}\right) + \left\{61 \times \text{pH} - 59.88 \times \log \frac{[NH_4^+]}{[NO_x^-]}\right\}$$

2.5 Test analysis

The system was monitored using chemical and physical analyses of influent and effluent samples according to Standard Methods for the Examination of Water and Wastewater. The parameters analyzed include: pH and ORP measurements, chemical oxygen demand (COD), nitrate ($N–NO_3^-$) and ammonium (NH_4^+) analyses. pH and oxidation–reduction potential (ORP) were monitored using a Mettler Toledo pH 2100 sensor. The pH measurement sensitivity is ±0.01 units, and the ORP detection range is ±1200 mV, enabling accurate environmental monitoring during anaerobic processes. The COD was analyzed using Method 5220 D, with detection ranges adaptable for high (0–1500 mg L^{-1}) and low (0–150 mg L^{-1}) concentrations. This dual range allowed the precise monitoring of organic load variations in the reactor. Nitrate concentrations were measured using the 4500 A Standard Method with UV absorption at 220/270 nm, providing a detection limit of approximately 0.1 mg L^{-1}. The ammonium levels were determined *via* the phenate method at 640 nm with a sensitivity threshold of 0.02 mg L^{-1}, which ensured accurate detection under fluctuating influent characteristics. These specific detection limits and equipment sensitivities ensure a high level of accuracy in measuring environmental conditions and pollutant levels throughout the experimental setup, supporting reliable monitoring and reproducibility.

3 Results and discussion

3.1 Synthesis of hydrogel carrier

The HG carrier was obtained by the radio-induced polymerization of hydroxyethyl methacrylate (HEMA) and copolymerized with acrylamide (AA). The use of different ratios of HEMA and AA resulted in carriers with varying densities and swelling grades, depending on the percentage weight/weight of AA present in the dry HEMA. The results of the swelling of different compositions of HEMA/AA at 25 kGy are shown in Table 2.

The samples swelled in proportion to the increased AA content. The HEMA sample swelled up to double its weight, while the incorporation of 50% w/w of AA increased the weight by several times. This was due to the high formation and superficial charge of ammonium incorporated, which promoted water interaction. Swelling kinetics and diffusion mechanisms indicated that the water penetration followed first-order kinetics for the initial periods. These results are similar to those obtained by Karadağ and Turan.[19,34]

The HG 50/50 AA materials showed that they could be operated in the upper zone due to their low density. However, carriers obtained with high densities showed that this composition could be used in a bioreactor with a high fluidized regime, such as a fluidized bed. This is because this material should stay in the lower zone to avoid recirculation by tubes and pumps, and media with low density could be stratified by the same liquid, establishing three definite zones and behaving like a packed bed.

Microphotographs reveal that the dense materials have an elastomeric consistency when swelled in water, as shown in the additional figure. In this figure, it is possible to see the biofilm in contact with the hydrogel, which could be due to a biocompatibility process.

The microorganisms were mainly *Pseudomonas* (1–2 μm), which adhered to the carrier surface. Culture samples were cultivated in nutritive agar and EMB (Levine). The colonies were stained by Gram Tinction and then, were analyzed using API strips. The API-20E multitest system identified *Pseudomonas aeruginosa* (CODE: 1-353-575) with a high identification accuracy, and (CODE: 1-000-477) was compatible with *Xylosoxidans denitrificans*. Additional tests, such as the acetamide reaction, growth at 42 °C, the oxidative (OF) glucose test, and the production of pyocyanin pigment, support the identification of *P. aeruginosa*.

Microbial processes driving COD and nitrate removal involve aerobic and anaerobic degradation for COD, with aerobic heterotrophs oxidizing organic compounds under aerobic conditions, and anaerobic bacteria utilizing alternative electron acceptors in anaerobic environments. For nitrate removal, denitrifying bacteria sequentially reduce nitrate to nitrogen gas under anaerobic conditions.

3.2 Bioreactor configuration and operation modes

3.2.1 Packed-bed bioreactor (PBBR) *vs.* fluidized-bed bioreactor (FBBR) – Peclet number and HRT. Fig. 3 illustrates the relationship between the hydraulic retention time (HRT) and the nitrate removal efficiency in the packed-bed bioreactor (PBBR) for different initial nitrate concentrations (125, 250, 500, and 1000 mg L^{-1} $N–NO_3^-$). To achieve 90% nitrate removal, HRTs of approximately 10 hours were required for 1000 mg L^{-1} $N–NO_3^-$, while significantly longer HRTs (up to 5 days) were necessary for lower initial nitrate concentrations (500 and 250 mg L^{-1} $N–NO_3^-$). This trend suggests that the treatment efficiency decreases at lower contaminant concentrations due to reduced substrate availability for microbial activity.

It was observed that biofilm formation on the polycarbonate packing material was initially slow. However, once established, the biofilm exhibited excellent denitrification performance. The large surface area provided

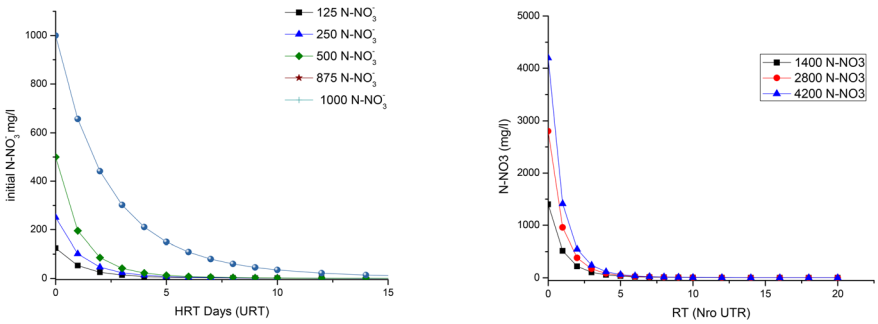

Fig. 3 Denitrification performance in the function of HRT at PBBR.

by the polycarbonate plates likely facilitated the development of a robust and active biofilm.

For the fluidized-bed bioreactor (FBBR), a constant flow rate of 0.0029 m^3 h^{-1} was maintained to ensure adequate fluidization of the carriers. Experiments were conducted with increasing nitrate concentrations (1400 to 4200 mg L^{-1}). Influent nitrate concentrations of 1400, 2800, and 4200 mg L^{-1} $N–NO_3^-$ were chosen to reflect realistic conditions in nuclear wastewater treatment and to evaluate the system's capacity to reduce the hydraulic retention time (HRT). Higher treatment rates in a mature biofilm allow for smaller reactor sizes or shorter treatment times, optimizing the system's efficiency and scalability.

Fig. 3 shows the influence of nitrate concentration on the HRT for nitrate levels of 125, 250, 500, and 1000 mg l^{-1} $N–NO_3^-$ in the PBBR, as well as for levels of 1400, 2800 and 4200 in the PBBR. To achieve 90% efficiency at a PBBR concentration of 1000 mg l^{-1} $N–NO_3^-$, approximately 10 hours are required, whereas for 750 mg l^{-1} $N–NO_3^-$, the time extends to nearly 5 days, similar to the period for 500 mg l^{-1} $N–NO_3^-$. At lower concentrations, treatment processes are less efficient due to reduced contaminant levels available for reaction with treatment agents. This necessitates a longer time for adequate chemical reactions to occur, achieving desired contaminant removal. For initial concentrations of 250 and 125 mg l^{-1} $N–NO_3^-$, there is an approximate reduction of 3 days in residence time. This signifies that at higher concentrations, particularly at 1000 mg l^{-1} $N–NO_3^-$, the retention periods escalate twofold to achieve commensurate efficacy in the treatment process. Thus, in order to sustain a conversion efficiency of 90%, it is advisable for the system to manage concentrations not exceeding 1000 ppm.

It seems that the biofilm formation on the polycarbonate plates took a significant amount of time to occur, but once established, the denitrification process showed excellent performance. The large surface area of the polycarbonate plates may have facilitated the formation of a robust biofilm that was able to efficiently carry out the desired process.

The provided information states that the Peclet number ranged from 4.62 to 5.1 within the tested nitrate concentration range of 125–1000 mg L^{-1} $N–NO_3^-$. The high Peclet number suggests that the reactor design effectively minimizes axial dispersion, which is crucial for achieving high conversion rates in many bioreactor applications.

This characteristic is beneficial for many bioreactor applications, particularly those that require high conversion rates and minimal contact between effluent and influent streams. However, it seems that clogging may have been an issue that impeded circulation at 400 h, which may have negatively impacted the performance of the bioreactor. As a result, further testing with a packed-bed bioreactor has not been conducted.

For FFBR, the flux was 0.0029 m^3 h^{-1} to maintain the fluidification; however, the nitrate concentration was increased from 1400 to 4200 mg l^{-1}. The FBBR demonstrated high-nitrate removal efficiencies across the tested concentration range. The high Peclet number observed in the FBBR (range: 4.62–5.1) indicates that the reactor exhibited minimal axial dispersion, promoting efficient flow through the bed and minimizing backmixing. This characteristic is beneficial for maximizing the residence time of the substrate within the reactor and enhancing the overall treatment efficiency.

The proposed system combines the advantages of fixed-bed biofilm reactors (PBBRs), which provide a high surface area for biofilm formation even under low Reynolds or laminar flow conditions, with those of fluidized-bed reactors (FBBR), which offer excellent mixing and mass transfer due to their dynamic fluid motion. However, conventional PBBR systems are prone to clogging, while FBBR systems are limited by carrier loading capacity and often struggle to support robust biofilm formation. To address these limitations, this study utilizes variable-density carriers, which increase loading capacity and prevent excessive biofilm accumulation through carrier collisions. This hybrid approach enhances both efficiency and practicality, enabling efficient fluidization at low-flow rates while mitigating clogging issues commonly observed in conventional systems.

3.2.2 Fluidized-bed bioreactor (FBBR) denitrification of nuclear effluents. It appears that the fluidized-bed reactor has advantages over the other types of bioreactors, particularly in avoiding issues related to clogging and channeling that may be encountered in other systems. The acclimatization of the column started with a synthetic medium containing methanol (200 ml/45 l equivalent to 0.1

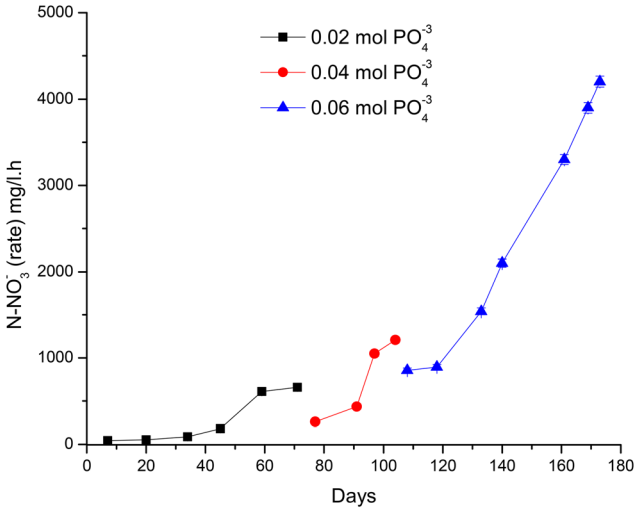

Fig. 4 Kinetic behavior of the culture at three different periods to check the development of the biofilms in a semi-continuous experiment to establish the capacities of maximum denitrification at different PO_4^{3-} concentrations.

M), potassium nitrate ($N–NO_3^-$ 1650 mg l^{-1}), and phosphoric acid 85% (35 ml l^{-1}), filling the column with the carrier to 90% capacity (30 × 30 × 30). Nitrite, a key intermediate in denitrification, was evaluated in laboratory tests. At pH < 7, low nitrite concentrations were detected, while at pH > 7.5, nitrite was absent, indicating rapid conversion to N_2. Given these results, nitrite monitoring was deemed unnecessary in full-scale experiments.

The reactor operated in a closed-loop batch system with recirculation to acclimate the biofilm. After 14 days, the concentration of $N–NO_3^-$ dropped to zero. The system can operate more efficiently and effectively, reducing the need for frequent maintenance and allowing for longer operating times between cleanings and replacements of the packing material. Ultimately, this can lead to cost savings and better system performance, as shown in Fig. 4. The process continues with a 24 h HRT. Fig. 6 shows the denitrification process and different nutrient (PO_4^{3-}) fluxes within the fluidized-bed reactor.

In the first period, the initial of $KH_2PO_4^{3-}$ was 0.02 M, with an initial nitrate concentration of 1400 mg l^{-1} $N–NO_3^-$. The maximum rate reached was 600 mg l^{-1} $N–NO_3^-$ over 60 days.

Shear forces play a critical role in maintaining biofilm stability and reactor performance. In fluidized-bed reactors (FBBRs), shear stress generated by particle collisions and fluid turbulence prevents excessive biofilm accumulation, ensuring a balance between biofilm growth and detachment. This dynamic enhances mass transfer efficiency and minimizes clogging. In contrast, fixed-biofilm reactors (PBBRs) experience a lower shear stress, leading to thicker biofilms, clogging, and reduced hydrodynamic efficiency.

Studies have identified critical shear thresholds (*e.g.*, 0.1–0.5 Pa) necessary for effective biofilm detachment while maintaining active biomass.[34] These findings underscore the importance of shear forces in optimizing reactor design and performance, particularly for treating high-nitrate and uranium-contaminated effluents.

In the second instance, the concentration of the $KH_2PO_4^{3-}$ in the media was increased to 0.01 M. Establishing that there was a limitation in the amount of phosphates available for suspended biomass retained by HG may have played an important role in the observed differences in process performance, particularly with regard to the biomass composition ($CH_{1.7}O_{0.5}N_{0.2}P_{0.01}$). The initial concentration of $N–NO_3^-$ was 2800 mg/l/day and the maximum velocity achieved by the removal of the biofilm was approximately 1200 $N–NO_3^-$ mg/l/day.

Enhanced denitrification may result from an increased capacity for active biofilm formation that enhances performance, avoiding clogging and phosphorus limitation. It seems that it requires the shortest times to achieve almost complete nitrate removal observed at an efficiency up to 96.6%. Fluidization facilitates solid–liquid mass transfer despite having a Pe > 1.5 (5), which promotes good contact. Additionally, fluidization eliminates preferential flow paths, prevents bed clogging, and reduces the need for frequent cleaning or replacement of the packing material, which is another common problem encountered in packed-bed reactors.

The HRT and the properties of the denitrification reaction were obtained from empirical data through the first derivative of a dimensionless number, as shown in the Materials and methods section. The values were calculated by the first derivate of the denitrification rate, as shown in Table 3.

The nitrate removal efficiency reached high values of around 95% within a short time. The application of slow agitation in the biological packet-bed ensured high-nitrate conversion at the same time, which shows that the slow agitation of biological Slow Agitation Media has a positive effect on nitrate removal. A Peclet number of 4 suggests that diffusion is greater than the rate of convective transport in the PBBR system; however, the flow was piston-like.

The slow agitation in the FBBR was effective in ensuring high-nitrate conversion while avoiding the clogging formation. This was achieved through a combination of low Reynolds number and high residence times (RTs).

In the upflow reactors, the hydrogels had a differential distribution. The carriers with a HEMA composition were scattered in the lower zones of the column, while the hydrogels with HEMA 50% AA were promoted and "washed from the column", eventually settling in the upper zones. When all three types of hydrogels were incorporated into the

Table 3 Hydrodynamic parameters in FBBRs and PBBRs

Flux (l min^{-1})	0.0029
Large (m)	1.155
Peclet no.	4

column, they were distributed in two zones: the low zone consisted of HEMA, while the middle zone contained HEMA + 25% AA and HEMA + 50% AA in equal proportions (Fig. 4).

These findings suggest that the distribution of hydrogels in the column can have a significant impact on the performance of the system, and careful consideration of their placement may be necessary to optimize the process for specific applications.[35]

The hydrodynamic carriers' properties obtained in FBBRs are presented in Table 4 and the results are given as a graph in Fig. 5.

The head loss in FBBRs is shown in Fig. 5. The inflexion points were 2, 2.5 and 3 m s^{-1}, respectively, which are low values to operate a FBBR, to achieve a great quantity of HG (Table 5), and therefore, for a superficial area to biomass adhesion. The Reynolds number (R_2) was 117 893 (turbulent), the velocity (V) was 0.79 m s^{-1} and the Darcy friction factor (f_D) was 0.017.

The differences between fluidized-bed bioreactors (FBBRs) and packed-bed bioreactors (PBBRs) stem from their operational principles and design objectives. PBBRs aim to provide a large surface area to support biomass through laminar flux, enhancing media mass transfer. Conversely, FBBRs feature a smaller superficial area but operate under turbulent flux conditions, which increase the mass transfer rates and prevent the formation of biofilms.

In PBBRs, the emphasis is on maximizing the surface area available for biomass attachment, facilitating efficient substrate utilization and biological treatment. This configuration promotes laminar flow, ensuring thorough contact between the substrate and the biofilm for effective pollutant removal.

However, FBBRs prioritize turbulent flow to enhance the mass transfer rates and prevent biofilm formation. The fluidization of particles in FBBRs promotes agitation and mixing, ensuring the uniform distribution of substrates and preventing the accumulation of biomass on the reactor surface.

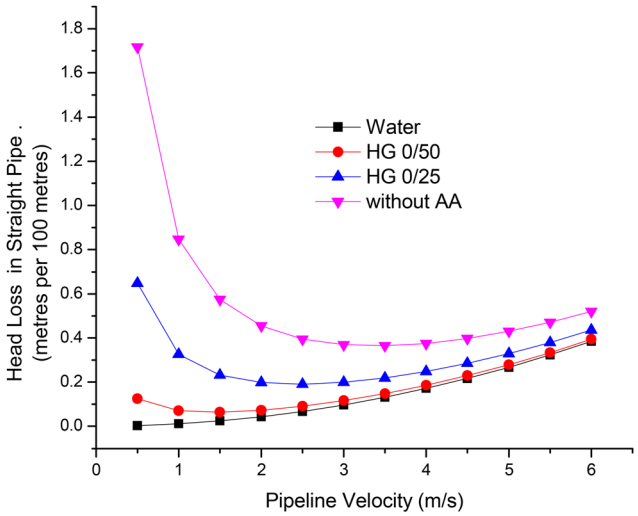

Fig. 5 Head loss in FBBR.

Table 5 Minimum, medium and maximum (cm) determined values of HG in columns

HG type	Minimum	Medium	Maximum
Min HG	1	5	18
Max HG	37	39	40
Min HG50	75	90	95
Max HG50	110	110	110
Min HG25	56	58	58
Min Hg25	20	78.5	81

These distinctions in operational principles contribute to the overall performance of each bioreactor type. PBBRs excel in providing extensive surface area for biomass attachment, facilitating efficient substrate utilization and pollutant removal. In contrast, FBBRs leverage turbulent flow to enhance mass transfer rates, preventing biofilm formation and maintaining operational efficiency.

Table 4 Hydrodynamic characteristics of HG carriers

HG HEMA only		
Drag coefficient at terminal settling velocity (C_D^*)	—	0.04
Particle Reynolds number at terminal settling velocity ($R^*_{particle}$)	—	0.000
Particle terminal settling velocity (v_T)	m s^{-1}	6.12×10^2
HG HEMA 50/AA25		
Particle drag coefficient at terminal settling velocity (C_D^*)	—	0.25
Particle Reynolds number at terminal settling velocity ($R^*_{particle}$)	—	0.001
Particle terminal settling velocity (v_T)	m s^{-1}	6.1
HG HEMA 50/AA25		
Particle drag coefficient at terminal settling velocity (C_D^*)	—	0.18
Particle Reynolds number at terminal settling velocity ($R^*_{particle}$)	—	0.008
Particle terminal settling velocity (v_T)	m s^{-1}	1.47×10^1

Hybrid packed-bed bioreactors (PBBs) with HG biofilm carriers emerge as simple and highly productive options with favorable hydrodynamic characteristics that promote biofilm performance at the bench scale. These systems offer advantages such as low-cost catalyst carriers, high biomass retention and reduced clogging, they can be operated for extended periods, reducing process costs.

When comparing fluidized-bed bioreactors (FBBRs) with other systems, FBBRs are particularly suitable for environmental bioremediation. Successful scale-up can be achieved by maintaining similar chemical and physical conditions in both scales while using carriers with different densities. However, further research is needed to assess pilot-scale feasibility and improve the anaerobic digestion system for bacterial adhesion in FBBRs.

The disadvantages of FBBRs include reactor size limitations due to the height-to-diameter ratio and high energy requirements resulting from high recycle ratios. Considering the beneficial characteristics of FBBRs, they are expected to become increasingly applied in wastewater treatment, as well as in many physical and chemical process applications, such as incineration, phosphate recovery, and advanced oxidation processes.

FBBRs have been widely used for anaerobic bioreactors. The system consists of coated particles in wastewater, which are sufficiently fluidized to keep.[36] The support materials of FBBRs normally have extremely specific surfaces, achieving elimination levels in a shorter time than conventional biological treatment. This is because fluidization maximizes contact surface between pollutants and the biofilm on support materials. The fluidized-bed bioreactor (FBBR) prevents clogging by maintaining biofilm stability through continuous carrier movement and fluid turbulence, unlike packed-bed bioreactors (PBBRs), where biofilm accumulation leads to clogging and dead zones. Additionally, the turbulent flow in FBBRs enhances mass transfer by promoting uniform mixing and efficient nutrient diffusion, resulting in higher denitrification rates. These advantages make FBBRs more effective for treating high-nitrate nuclear effluents.

These results demonstrate that the fluidized bioreactor, with hybrid behavior, offers stability, avoids clogging formation, increases the operation efficiency of the activated sludge process, and provides advantages over stirred tanks. This new innovative type of bioreactor combines the high availability of catalytic converters from the packed bed, avoiding excessive formation of biofilm and plugs, with lower power consumption than the fluidized bed.

The chosen configuration bears similarities to MBBRs, under agitation with paddles and aerobic conditions. When compared with the MBBR, we observe similar performances to those obtained in our system. For instance, Dong *et al.*[37] achieved an HRT of 10–18 with an efficiency of 90% using ceramic carriers with a density of 1, while Hou[22] achieved an HRT of 5 with an efficiency close to 61% using the MBBR with carriers made of PP and PS.

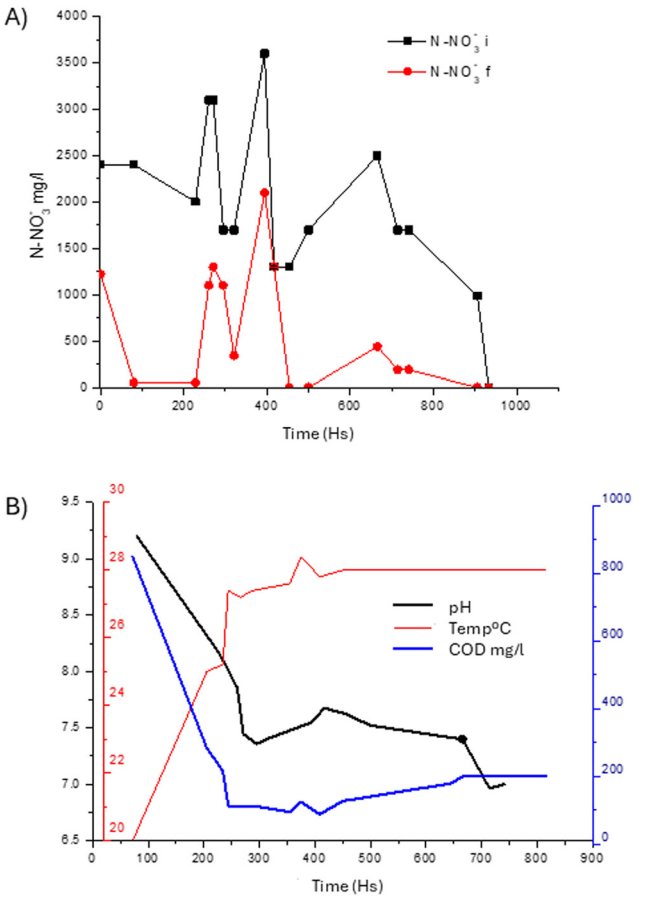

Fig. 6 Denitrification process in FBBRs: A) denitrification performance and B) monitored parameters: pH, *T* (°C), and COD.

The effluent was equalized and subjected to aerobic treatment to remove ammonia, before transferring to the FBBR for the monitoring of ORP and pH levels. Fig. 6 displays the denitrification performance.

The average denitrification rate was 1631 (±380) mg/l $N–NO_3$/day. Between 200 and 400 hours, it was necessary to incorporate methanol because the stoichiometry ratio of C/N was low. Then, the system was operated with an excess of carbon. Despite the pre-established acclimatization phase, the cultivation exhibited a delay of over 72 hours in initiating the intended process. Furthermore, observations at 250 and 400 hours revealed an elevation in the load to 3000 mg l^{-1}, yet the process exhibited inefficiency. This inefficacy could be attributed to the adverse toxic attributes of the effluent and the resulting inhibitory effects. Subsequent to a prolonged duration, the system finally attained a stable operational state. Therefore, a strategic decision was made to cap the maximum load at 2000 mg l^{-1}.

In contrast, Rout *et al.* showed the efficacy and efficiency in nitrogen and COD elimination when operating at a C/N ratio of 5, impeding the nitrification process crucial for ammonium nitrogen conversion. At a COD/NO_3^- ratio of 2.5, a strategy was observed that partially enhanced nitrate

removal efficiency while simultaneously reducing microbial diversity. Similarly, hydraulic retention time of 32 hours and an influent nitrate concentration of 50 mg L^{-1} emerge as the quintessential recipe for fostering elevated nitrate removal rates, removing 99.4%.[37,38] Strategic regulation of the carbon-to-nitrogen ratio within freshwater ponds presents a promising avenue for bolstering the nitrate removal efficacy while mitigating nitrite accumulation, thereby mitigating environmental adversities.

PBBRs excel in providing surface area for biomass attachment, while FBBRs enhance mass transfer rates and prevent biofilm formation. Considerations include reactor size, energy requirements, and operational stability. Despite challenges, FBBRs show promise for wastewater treatment and other processes, fostering further research for optimization and broader application. This potential extends to biotechnology processes involving enzyme or eukaryotic cell immobilization, as low-flow conditions minimize the risk of cell damage.

Advancements in wastewater treatment, particularly in the context of uranium industry wastewater treatment, have been really significant. Various technologies and methods have been developed to address the challenges associated with treating radioactive wastewater effectively; however, very few treatments have demonstrated efficient and robust advances. Some key contributions to advancements in wastewater treatment, especially in uranium industry wastewater treatment, included chemical precipitation method, ion exchange, evaporation concentration, adsorption, precipitation, biotechnology, membrane separation, and photocatalysis. However, these technologies have a high energy demand, the use of a low heat rate when processing the residual liquid, rapid corrosion of the equipment to be used, strict control of the system temperature and possibility of secondary contamination. Indeed, the advancements showed in this work contribute significantly to the field of wastewater treatment, especially in the uranium industry, by offering more efficient, cost-effective, and environmentally friendly solutions for treating radioactive wastewater.

The innovative bioreactor system developed in this study demonstrates strong potential for real-world applications, particularly in treating complex effluents with high-nitrate and uranium concentrations. Its scalability is supported by a modular design, high carrier load capacity, energy efficiency, and adaptability to variable effluent compositions. These features make it a promising solution for large-scale industrial wastewater treatment, contributing to sustainable water management and environmental protection.

4 Conclusions

When compared with other systems, HG carriers emerge as highly productive, cost-effective options with favorable hydrodynamic characteristics. Based on the results, we conclude that the fluidized-bed bioreactor (FBBR) with HG biofilm carriers demonstrated superior performance to the packed-bed bioreactor (PBBR) in terms of nitrate and COD removal efficiencies. The FBBR's fluidized design provided enhanced mass transfer, minimized clogging through uniform biofilm distribution, and showed greater resilience to variable influent conditions. These results highlight the FBBR with HG carriers as a robust option for industrial applications, particularly in treating high-contaminant and fluctuating wastewater sources. Comparing fluidized-bed bioreactors with other systems, the FBBR is suitable for environmental bioremediation. Successful scale-up can be achieved by maintaining similar chemical and physical conditions in both scales while using carriers with different densities. Further research is needed to assess pilot-scale feasibility and improve the anaerobic digestion system for bacterial adhesion.

Future research should focus on several key areas to advance the pilot-scale feasibility of these bioreactor systems. First, there is a need for comprehensive studies to optimize the operating parameters and design configurations of PBBRs and FBBRs to ensure efficient performance and scalability into the long-term stability and robustness of these systems, which are essential to assess their performance under varying environmental conditions and fluctuating influent characteristics. Understanding the dynamics of FBBRs over extended operational periods is crucial for reliable and sustainable operation at the pilot scale. Additionally, further exploration is needed to improve bacterial adhesion. Strategies such as surface modification of carrier materials may be effective. Furthermore, interdisciplinary research efforts integrating bioreactor engineering, microbiology, and environmental science will be instrumental in addressing the complex challenges associated with scaling up FBBRs for practical applications.

Data availability

The data supporting the findings of this study, including the synthesis parameters of floating carriers, hydrodynamic properties, and bioreactor performance metrics, are available within the manuscript and materials. Additional raw data, experimental protocols, and detailed performance results for nitrate and COD removal, as well as uranium-contaminated wastewater treatment, can be obtained from the corresponding author upon reasonable request. This ensures transparency and facilitates further research to build upon our findings in the field of sustainable water treatment.

Author contributions

Conceptualization: V. M. and P. B.; methodology: V. M. and P. B.; investigation: V. M. and P. B.; writing – original draft preparation: V. M. and P. B.; writing – review and editing: V. M., P. B. and R. M. All authors have read and agreed to the published version of the manuscript.

Conflicts of interest

There are no conflicts to declare.

Acknowledgements

This research received no external funding from the National Commission of Atomic Energy.

References

1 D. Jeong, K. Cho, C.-H. Lee, S. Lee and H. Bae, Integration of Forward Osmosis Process and a Continuous Airlift Nitrifying Bioreactor Containing PVA/Alginate-Immobilized Cells, *Chem. Eng. J.*, 2016, **306**, 1212–1222, DOI: **10.1016/j.cej.2016.08.050**.

2 X. Quan, K. Huang, M. Li, M. Lan and B. Li, Nitrogen Removal Performance of Municipal Reverse Osmosis Concentrate with Low C/N Ratio by Membrane-Aerated Biofilm Reactor, *Front. Environ. Sci. Eng.*, 2018, **12**, 5, DOI: **10.1007/s11783-018-1047-6**.

3 Zero Liquid Discharge (ZLD), Available online: **https://condorchem.com/en/zld/**, (accessed on 6 October 2018).

4 N. Roch, Analysis of Ammonia Removal From Wastewater Market: Feasibility of Saltworks Introducing New Technology, *Master Thesis MBA*, Simon Fraser University, Canada, 2015.

5 K. Dhangar and M. Kumar, Tricks and Tracks in Removal of Emerging Contaminants from the Wastewater through Hybrid Treatment Systems: A Review, *Sci. Total Environ.*, 2020, **738**, 140320, DOI: **10.1016/j.scitotenv.2020.140320**.

6 J. Schoeman and A. Steyn, Nitrate Removal with Reverse Osmosis in a Rural Area in South Africa, *Desalination*, 2003, **155**, 15–26.

7 M. Żołnierczyk and K. Barbusiński, Physicochemical Methods Of Nitrates Removal From Wastewater, *Architecture, Civil Engineering, Environment*, 2019, **12**, 153–159, DOI: **10.21307/acee-2019-046**.

8 S. Morris, G. Garcia-Cabellos, D. Ryan, D. Enright and A.-M. Enright, Low-Cost Physicochemical Treatment for Removal of Ammonia, Phosphate and Nitrate Contaminants from Landfill Leachate, *J. Environ. Sci. Health, Part A: Toxic/Hazard. Subst. Environ. Eng.*, 2019, **54**, 1233–1244, DOI: **10.1080/10934529.2019.1633855**.

9 G. A. Ekama, REVIEW Recent Developments in Biological Nutrient Removal, *Water SA*, 2015, **41**(4), 515–524, DOI: **10.4314/wsa.v41i4.11**.

10 Z. Liang, Z. Shujun, P. Yongzhen, H. Xiaoyu and G. Yiping, Nitrogen Removal Performance and Microbial Distribution in Pilot- and Full-Scale Integrated Fixed-Biofilm Activated Sludge Reactors Based on Nitritation-Anammox Process, *Bioresour. Technol.*, 2015, **196**, 448–453, DOI: **10.1016/j.biortech.2015.07.090**.

11 H. T. Le, N. Jantarat, W. Khanitchaidecha, K. Ratananikom and A. Nakaruk, Performance of Nitrogen Removal in Attached Growth Reactors with Different Carriers, *J. Water Reuse Desalin.*, 2018, **8**, 331–339, DOI: **10.2166/wrd.2017.182**.

12 W. Wu, F. Yang and L. Yang, Biological Denitrification with a Novel Biodegradable Polymer as Carbon Source and Biofilm Carrier, *Bioresour. Technol.*, 2012, **118**, 136–140, DOI: **10.1016/j.biortech.2012.04.066**.

13 M. Ahmad, S. Liu, N. Mahmood, A. Mahmood, M. Ali, M. Zheng and J. Ni, Effects of Porous Carrier Size on Biofilm Development, Microbial Distribution and Nitrogen Removal in Microaerobic Bioreactors, *Bioresour. Technol.*, 2017, **234**, 360–369, DOI: **10.1016/j.biortech.2017.03.076**.

14 J. B. van Lier, F. P. van derZee, C. T. M. J. Frijters and M. E. Ersahin, Celebrating 40 Years Anaerobic Sludge Bed Reactors for Industrial Wastewater Treatment, *Rev. Environ. Sci. Biotechnol.*, 2015, **14**, 681–702, DOI: **10.1007/s11157-015-9375-5**.

15 J. R. Howard, *Fluidized Bed Technology: Principles and Applications*, CRC Press, Bristol, New York, 1st edn, 1989, ISBN 978-0-85274-055-2.

16 S. P. Burghate and D. N. W. Ingole, Fluidized Bed Biofilm Reactor – A Novel Wastewater Treatment Reactor, Available online: /paper/Fluidized-Bed-Biofilm-Reactor-%E2%80%93-A-Novel-Wastewater-Burghate-Ingole/d8b37397868550edac63c50393a4e3b107688f64, (accessed on 3 December 2018).

17 Y. Dong, S.-Q. Fan, Y. Shen, J.-X. Yang, P. Yan, Y.-P. Chen, J. Li, J.-S. Guo, X.-M. Duan and F. Fang, *et al.*, A Novel Bio-Carrier Fabricated Using 3D Printing Technique for Wastewater Treatment, *Sci. Rep.*, 2015, **5**, 12400, DOI: **10.1038/srep12400**.

18 G. Luo, Z. Liu, J. Gao, Z. Hou and H. Tan, Nitrate Removal Efficiency and Bacterial Community of Polycaprolactone-Packed Bioreactors Treating Water from a Recirculating Aquaculture System, *Aquacult. Int.*, 2018, **26**, 773–784, DOI: **10.1007/s10499-018-0251-5**.

19 E. Karadağ, Ö. B. Üzüm, D. Saraydın and O. Güven, Swelling Characterization of Gamma-Radiation Induced Crosslinked Acrylamide/Maleic Acid Hydrogels in Urea Solutions, *Mater. Des.*, 2006, **27**, 576–584, DOI: **10.1016/j.matdes.2004.11.019**.

20 E. Kardena, S. L. Ridhati and Q. Helmy, Molecular Imprinted Hydrogel Polymer (MIHP) as Microbial Immobilization Media in Artificial Produced Water Treatment, *IOP Conf. Ser.: Earth Environ. Sci.*, 2018, **106**, 012088, DOI: **10.1088/1755-1315/106/1/012088**.

21 M. Maaz, M. Yasin, M. Aslam, G. Kumar, A. E. Atabani, M. Idrees, F. Anjum, F. Jamil, R. Ahmad and A. L. Khan, *et al.*, Anaerobic Membrane Bioreactors for Wastewater Treatment: Novel Configurations, Fouling Control and Energy Considerations, *Bioresour. Technol.*, 2019, **283**, 358–372, DOI: **10.1016/j.biortech.2019.03.061**.

22 Y. Hou, M. Liu, X. Tan, S. Hou and P. Yang, Study on COD and Nitrogen Removal Efficiency of Domestic Sewage by Hybrid Carrier Biofilm Reactor, *RSC Adv.*, 2021, **11**, 27322–27332, DOI: **10.1039/D1RA03286K**.

23 M. Aslam, P. Yang, P.-H. Lee and J. Kim, Novel Staged Anaerobic Fluidized Bed Ceramic Membrane Bioreactor: Energy Reduction, Fouling Control and Microbial Characterization, *J. Membr. Sci.*, 2018, **553**, 200–208, DOI: **10.1016/j.memsci.2018.02.038**.

24 Q. Ying, C. Xiao-tong, L. Bing, F. Gen-na, W. Yang, S. You-lin, L. Zhen-ming, T. Ya-ping and T. Chun-he, The Conceptual Flowsheet of Effluent Treatment during Preparing Spherical Fuel Elements of HTR, *Nucl. Eng. Des.*, 2014, **271**, 189–192, DOI: **10.1016/j.nucengdes.2013.11.030**.

25 How Uranium Ore Is Made into Nuclear Fuel - World Nuclear Association, Available online: **https://www.world-nuclear.org/nuclear-basics/how-is-uranium-ore-made-into-nuclear-fuel.aspx**, (accessed on 27 July 2019).

26 M. A. Tadda, R. Altaf, M. Gouda, P. R. Rout, A. Shitu, Z. Ye, S. Zhu and D. Liu, Impact of Saddle-Chips Biocarrier on Treating Mariculture Wastewater by Moving Bed Biofilm Reactor (MBBR): Mechanism and Kinetic Study, *J. Environ. Chem. Eng.*, 2021, **9**, 106710, DOI: **10.1016/j.jece.2021.106710**.

27 J. C. Cuggino, Síntesis de Para Su Posible Aplicación En La Liberación de Drogas Controladas, 16–17 Octubre 2008, *2° Encuentro de Jóvenes Investigadores en Ciencia y Tecnología de Materiales – Posadas – Misiones*, 2008.

28 M. K. Shahid, A. Kashif, P. R. Rout, M. Aslam, A. Fuwad, Y. Choi, J. R. Banu, J. H. Park and G. Kumar, A Brief Review of Anaerobic Membrane Bioreactors Emphasizing Recent Advancements, Fouling Issues and Future Perspectives, *J. Environ. Manage.*, 2020, **270**, 110909, DOI: **10.1016/j.jenvman.2020.110909**.

29 W. Kwak, P. R. Rout, E. Lee and J. Bae, Influence of Hydraulic Retention Time and Temperature on the Performance of an Anaerobic Ammonium Oxidation Fluidized Bed Membrane Bioreactor for Low-Strength Ammonia Wastewater Treatment, *Chem. Eng. J.*, 2020, **386**, 123992, DOI: **10.1016/j.cej.2019.123992**.

30 P. R. Rout, R. R. Dash, P. Bhunia and S. Rao, Role of Bacillus Cereus GS-5 Strain on Simultaneous Nitrogen and Phosphorous Removal from Domestic Wastewater in an Inventive Single Unit Multi-Layer Packed Bed Bioreactor, *Bioresour. Technol.*, 2018, **262**, 251–260, DOI: **10.1016/j.biortech.2018.04.087**.

31 P. R. Rout, R. R. Dash, P. Bhunia, E. Lee and J. Bae, Comparison between a Single Unit Bioreactor and an Integrated Bioreactor for Nutrient Removal from Domestic Wastewater, *Sustain. Energy Technol. Assess.*, 2021, **48**, 101620, DOI: **10.1016/j.seta.2021.101620**.

32 C.-N. Chang, H.-B. Cheng and A. C. Chao, Applying the Nernst Equation To Simulate Redox Potential Variations for Biological Nitrification and Denitrification Processes, *Environ. Sci. Technol.*, 2004, **38**, 1807–1812, DOI: **10.1021/es021088e**.

33 M. Venturini, A. Rossen, P. Bucci and P. Silva Paulo, Applying the Nernst Equation to Control ORP in Denitrification Process for Uranium-Containing Nuclear Effluent with High Loads of Nitrogen and COD, *Water*, 2022, **14**, 2227, DOI: **10.3390/w14142227**.

34 M. Turan, Mechanisms of Biofilm Detachment in Anaerobic Fluidized Bed Reactors, *Environ. Technol.*, 2000, **21**, 177–183, DOI: **10.1080/09593330.2000.9618898**.

35 J. Cuggino, Síntesis de Para Su Posible Aplicación En La Liberación de Drogas Controladas, in *Proceedings of the 2° Encuentro de Jóvenes Investigadores en Ciencia y Tecnología de Materiales – Posadas – Misiones*, 2008.

36 A. Venu Vinod and G. Venkat Reddy, Simulation of Biodegradation Process of Phenolic Wastewater at Higher Concentrations in a Fluidized-Bed Bioreactor, *Biochem. Eng. J.*, 2005, **24**, 1–10, DOI: **10.1016/j.bej.2005.01.005**.

37 Z. Dong, M. Lu, W. Huang and X. Xu, Treatment of Oilfield Wastewater in Moving Bed Biofilm Reactors Using a Novel Suspended Ceramic Biocarrier, *J. Hazard. Mater.*, 2011, **196**, 123–130, DOI: **10.1016/j.jhazmat.2011.09.001**.

38 P. R. Rout, P. Bhunia and R. R. Dash, Simultaneous Removal of Nitrogen and Phosphorous from Domestic Wastewater Using Bacillus Cereus GS-5 Strain Exhibiting Heterotrophic Nitrification, Aerobic Denitrification and Denitrifying Phosphorous Removal, *Bioresour. Technol.*, 2017, **244**, 484–495, DOI: **10.1016/j.biortech.2017.07.186**.